


"PHOTOIONIZATION OF HIGHLY CHARGED ARGON IONS AND THEIR DIAGNOSTIC LINES"

Sultana N. Nahar

Astronomy Dept, The Ohio State University

Columbus, Ohio, USA

"67th International Symposium on Molecular Spectroscopy"

Ohio State University, Columbus, Ohio, USA

June 18-22, 2012

Supports: DOE, NSF

Computations - Ohio Supercomputer Center

PHOTOIONIZATION:

$$\mathbf{PI:\quad Ar\ XVI + h\nu \rightleftharpoons Ar\ XVII + \epsilon \quad : RC}$$
$$\mathbf{PI:\quad Ar\ XVII + h\nu \rightleftharpoons Ar\ XVIII + \epsilon \quad : RC}$$

Inverse Process: Electron-Ion Recombination (RC)

Related through principle of detailed balance

- **Photoionization → Absorption lines**
- **Recombination → Emission Lines**
- **Diagnostics lines for astrophysical and laboratory plasmas**

These bound-free transitions may proceed as:

i) Photoionization (PI) & Radiative Recombination (RR) (1-step):

$$\mathbf{X^{+Z} + h\nu \rightleftharpoons X^{+Z+1} + \epsilon}$$

ii) Autoionization (AI) & Dielectronic Recombination (DR) (2-steps):

$$\mathbf{e + X^{+Z} \rightleftharpoons (X^{+Z-1})^{**} \rightleftharpoons \begin{cases} e + X^{+Z} & AI \\ X^{+Z-1} + h\nu & DR \end{cases}}$$

- ***The intermediate doubly excited autoionizing state*** $[(\mathbf{X^{+Z-1}})^{**}]$ ***introduces resonances***
- **RR and DR are inseparable in nature**
- **Unified Method considers both RR and DR**

X-RAYS IN SOLAR STORM

- Large amount of X-rays are emitted during solar storm
- The peak energies correspond to diagnostics lines of He- and Li-like ions

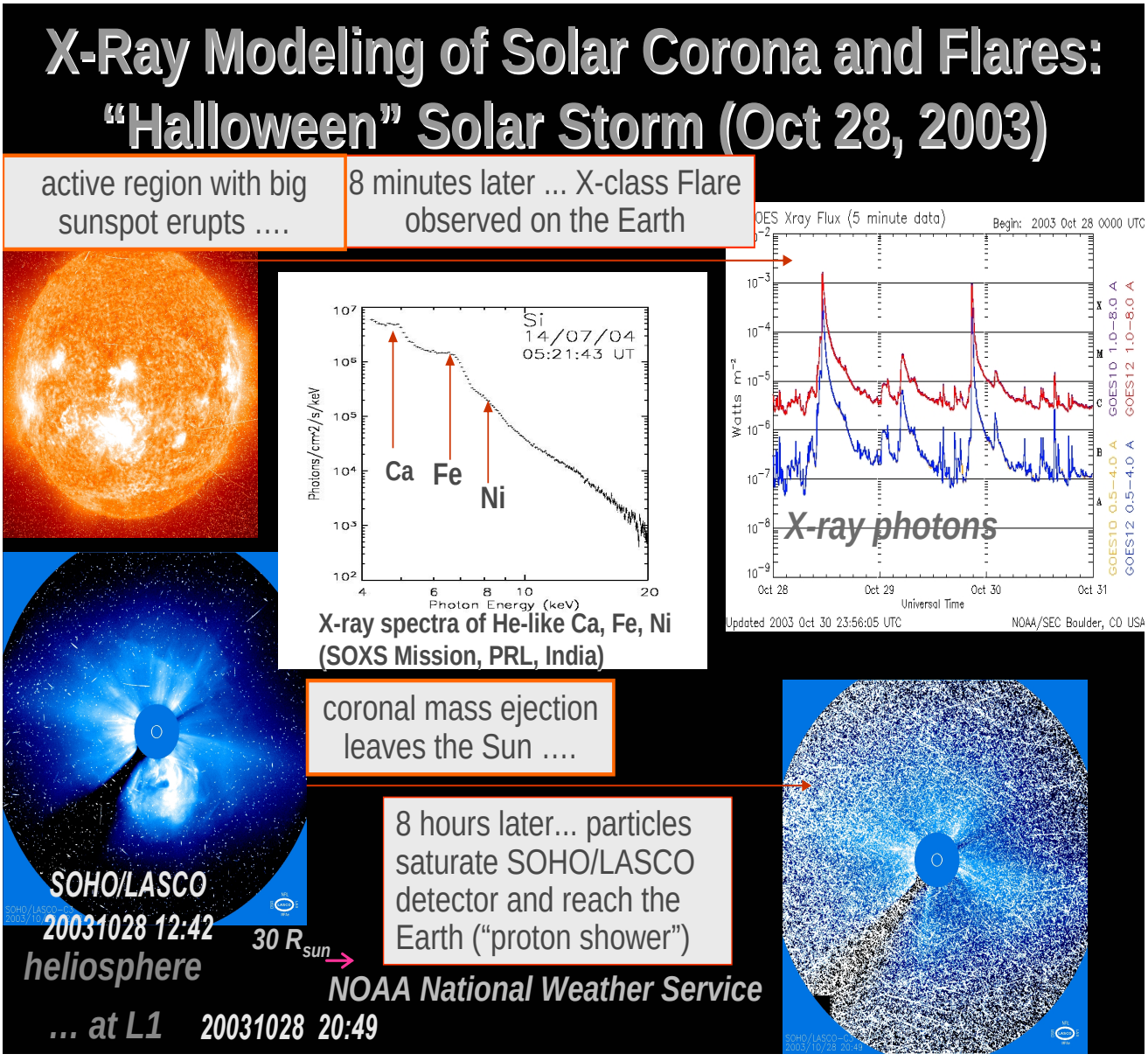

DIELECTRONIC SATELLITE (DES) LINES

• DES lines - common in (e+He-like ion) collision spectra forming 3-electron Li-like ion

• - produced by radiation damping of doubly excited autoionizing states in dielectronic recombination.

• Form below the excitation threshold of the core. Ex. KLL (1s2l2l') satellite lines are below the core excitation $1s^2(^1S_0) \rightarrow 1s2p(^1P^o_1)$ of w-line

• KLL (1s2l2l') complex introduces 22 DES lines (denoted as a,b,...,v - Gabriel 1972) as autoionizing states 1s2l2l' (1s2p2p, $1s2s^2$, $1s2p^2$) $\rightarrow$ $1s^22s(^2S_{1/2})$, $1s^22p(^2P^o_{1/2,3/2})$ bound states

Table: Dielectronic Satellite (DES) lines in in KLL resonance complex of a Li-like ion- Ar XVI

Key	Transition	E(eV)	Strength (eVcm2)
o	$1s2s^2(^2S_{1/2}) \rightarrow 1s^22p(^2P^o_{3/2})$	2162.13	1.1685E-20
p	$1s2s^2(^2S_{1/2}) \rightarrow 1s^22p(^2P^o_{1/2})$	2162.13	*
v	$1s2p^3P^o2s(^4P^o_{1/2}) \rightarrow 1s^22s(^2S_{1/2})$	2169.56	2.3222E-22
u	$1s2p^3P^o2s(^4P^o_{3/2}) \rightarrow 1s^22s(^2S_{1/2})$	2170.88	2.3656E-22
r	$1s2p^1P^o2s(^2P^o_{1/2}) \rightarrow 1s^22s(^2S_{1/2})$	2195.60	3.0728E-20
q	$1s2p^1P^o2s(^2P^o_{3/2}) \rightarrow 1s^22s(^2S_{1/2})$	2197.46	1.0379E-20
i	$1s2p^2(^4P_{1/2}) \rightarrow 1s^22p(^2P^o_{1/2})$	2204.44	1.9879E-22
h	$1s2p^2(^4P_{1/2}) \rightarrow 1s^22p(^2P^o_{3/2})$	2204.44	*
t	$1s2p^3P^o2s(^2P^o_{1/2}) \rightarrow 1s^22s(^2S_{1/2})$	2207.07	3.8027E-20
f	$1s2p^2(^4P_{3/2}) \rightarrow 1s^22p(^2P^o_{3/2})$	2205.94	2.7541E-22
g	$1s2p^2(^4P_{3/2}) \rightarrow 1s^22p(^2P^o_{1/2})$	2205.94	*
s	$1s2p^3P^o2s(^2P^o_{3/2}) \rightarrow 1s^22s(^2S_{1/2})$	2208.11	2.5439E-20
e	$1s2p^2(^4P_{5/2}) \rightarrow 1s^22p(^2P^o_{3/2})$	2208.11	*
k	$1s2p^2(^2D_{3/2}) \rightarrow 1s^22p(^2P^o_{1/2})$	2222.22	1.2508E-19
l	$1s2p^2(^2D_{3/2}) \rightarrow 1s^22p(^2P^o_{3/2})$	2222.49	1.0414E-20
d	$1s2p^2(^2P_{1/2}) \rightarrow 1s^22p(^2P^o_{1/2})$	2226.03	2.7841E-21
c	$1s2p^2(^2P_{1/2}) \rightarrow 1s^22p(^2P^o_{3/2})$	2223.03	2.7636E-19
j	$1s2p^2(^2D_{5/2}) \rightarrow 1s^22p(^2P^o_{3/2})$	2223.33	2.4523E-20
b	$1s2p^2(^2P_{3/2}) \rightarrow 1s^22p(^2P^o_{1/2})$	2229.43	2.5074E-20
a	$1s2p^2(^2P_{3/2}) \rightarrow 1s^22p(^2P^o_{3/2})$	2229.43	*
m	$1s2p^2(^2S_{1/2}) \rightarrow 1s^22p(^2P^o_{3/2})$	2245.35	3.8928E-20
n	$1s2p^2(^2S_{1/2}) \rightarrow 1s^22p(^2P^o_{1/2})$	2245.35	*

W, X, Y, Z LINES OF A He-LIKE ION

- These lines form form 1s-2s, 1s-2p transitions
- Prominent diagnostic lines

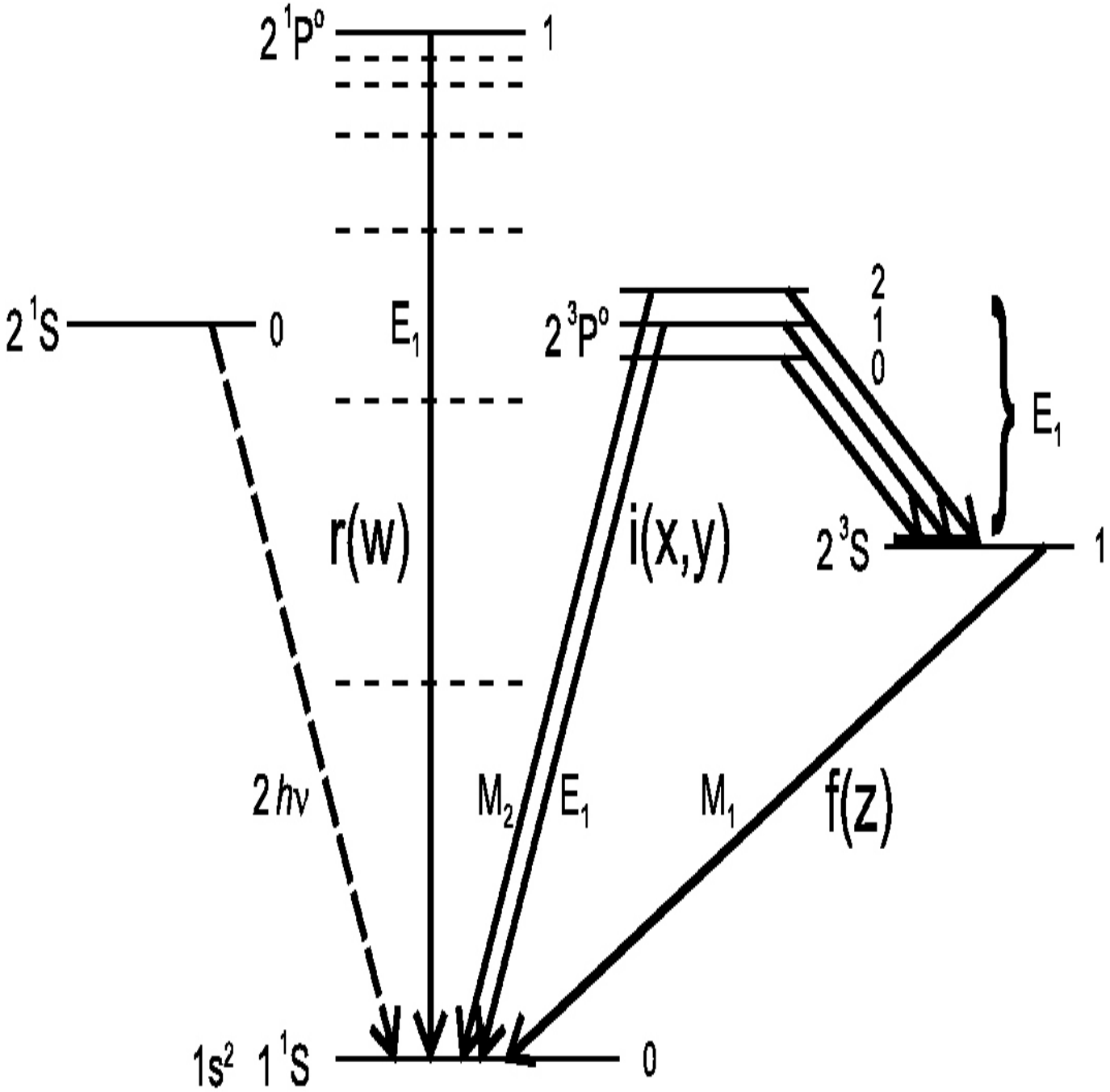

THEORY: Unified Method
(Nahar & Pradhan, PRL 1992, PRA 1994)

- Based on the ab initio close coupling (CC) approximation and R-matrix method - BPRM method
- Subsumes both RR and DR and calculates the total electron-ion recombination
- Considers infinite number of recombined states:

Advantages of the "Unified method":

- Provides self-consistent set of σ_{PI} and σ_{RC}; uses an identical wavefunction expansion for both the processes
- Provides "level-specific" recombination rate coefficients & photoionization cross sections for a large number of bound levels
- Provides unified total recombination spectra as seen in experiment
- Extension for Dielectronic Satellite (DES) Spectra(Nahar & Pradhan 2006) *Provides profiles, intensities and rates of DES lines*

COMPUTATIONS

Total wavefunction expansion in close coupling approximation:

$$\mathbf{\Psi_E(e+ion) = A\sum_i^N \chi_i(ion)\theta_i + \sum_j c_j\Phi_j(e+ion)}$$

χ_i → **target ion wavefunction,** Φ_j → **correlation functions of (e+ion),** θ_i → **wavefunction of the interacting electron (continuum or bound)**

• **The complex resonant structures in collisional and radiative processes are included through channel couplings.**

Table: Target levels: (Code: SUPERSTRUCTURE)

	Ar XVII			Ar XIX		
	level	E_o	E_c	level	E_o	E_c
1	$1s^2\ ^1S_0$	0.0	0.0	$1s\ ^2S_{1/2}$	0.0	0.0
2	$1s2s\ ^3S_1$	228.15016	228.38	$2p\ ^2P^o_{1/2}$	243.882	243.96
3	$1s2p\ ^3P^o_0$	1229.5280	229.69	$2s\ ^2S_{1/2}$	243.893	243.97
4	$1s2p\ ^3P^o_1$	229.57457	229.74	$2p\ ^2P^o_{3/2}$	244.235	244.31
5	$1s2s\ ^1S_0$	229.64803	229.79	$3p\ ^2P^o_{1/2}$	289.165	289.25
6	$1s2p\ ^3P^o_2$	229.77758	229.96	$3s\ ^2S_{1/2}$	289.169	289.25
7	$1s2p\ ^1P^o_1$	230.75281	230.97	$3d\ ^2D_{3/2}$	289.270	289.35
8	$1s3s\ ^3S_1$	270.03870	270.24	$3p\ ^2P^o_{3/2}$	289.270	289.35
9	$1s3p\ ^3P^o_0$	270.41843	270.61	$3d\ ^2D_{5/2}$	289.305	289.38
10	$1s3p\ ^3P^o_1$	270.43267	270.63	$4p\ ^2P^o_{1/2}$	305.000	305.08
11	$1s3s\ ^1S_0$	270.43506	270.61	$4s\ ^2S_{1/2}$	305.002	305.08
12	$1s3p\ ^3P^o_2$	270.49292	270.69	$4d\ ^2D_{3/2}$	305.044	305.12
13	$1s3d\ ^3D_2$	270.70333	270.90	$4p\ ^2P^o_{3/2}$	305.044	305.12
14	$1s3d\ ^3D_1$	270.70343	270.90	$4f\ ^2F^o_{5/2}$	305.059	305.14
15	$1s3d\ ^1D_2$	270.73840	270.94	$4d\ ^2D_{5/2}$	305.059	305.14
16	$1s3p\ ^1P^o_1$	270.75706	270.96	$4f\ ^2F^o_{7/2}$	305.066	305.15
17	$1s3d\ ^3D_3$	270.95804	270.92			

Ar XVII: correlations - $2s^2$,$2p^2$,$3s^2$, $3p^2$,$3d^2$,$2s2p$,$2s3s$,$2s3p$,$2s3d$, $2s4s$,$2s4p$,$2p3s$, $2p3p$,$2p3d$,$2p4s$,$2p4p$

λ_{nl} - 1.1(1s),0.99(2s),1.1(2p), 1(3s),1(3p),1(3d),1(4s),1(4p)

RESULTS

Ar XVI:

- **Number of bound levels $(1/2 \leq J \leq 17/2) = 98$ (NIST: smaller set)**
- **Total and partial σ_{PI} for 98 levels**
- **Level-specific α_{RC} for 98 levels**
- **Unified recombination cross sections**

Ar XVII:

- **Number of bound levels $(0 \leq J \leq 10) = 191$**
- **Total and partial σ_{PI} for all n$\leq$ 10 bound levels**
- **Level-specific α_{RC} for n$\leq$ 10 levels**
- **Unified recombination cross sections**

- **DES Lines: Dielectronic satellite spectrum of Ar XVI**

σ_{PI} OF GROUND LEVEL OF Ar XVI:

- a) Top Panel: Total (OP) - without the resonances
- b) Middle Panel: Total (Present) - Illustrates i) Resonances of n=2 complex ii) resonant effet is weaker with n=3 complex
- c) Bottom Panel: Partial - Similar to total except smooth at n=threshold as no contribution is added

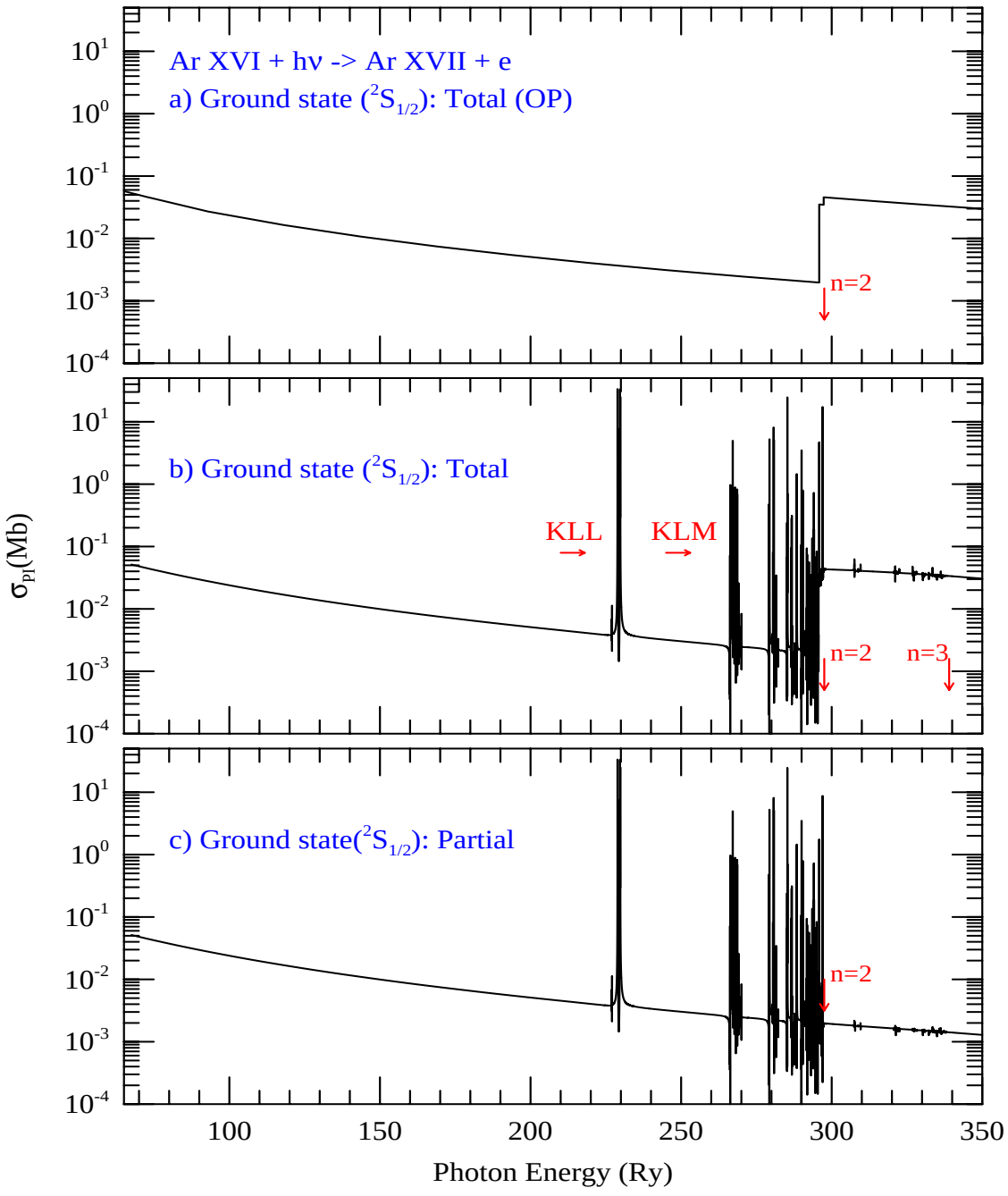

Ar XVI: PEC RESONANCES IN σ_{PI} OF EXCITED LEVELS

- **a-c): Total σ_{PI} of excited levels, $1s^2np(^2P^o_{1/2}$, $2 \leq n \leq 4$**
- **Excited levels show PEC or Seaton resonances due to dipole allowed transitions (arrows) to n=2 thresholds at about 230 Ry and n=3 thresholds at about 270 Ry**
- **Seaton resonances are wider than the narrow Rydberg resonances and hence contribute more at high temperatures**

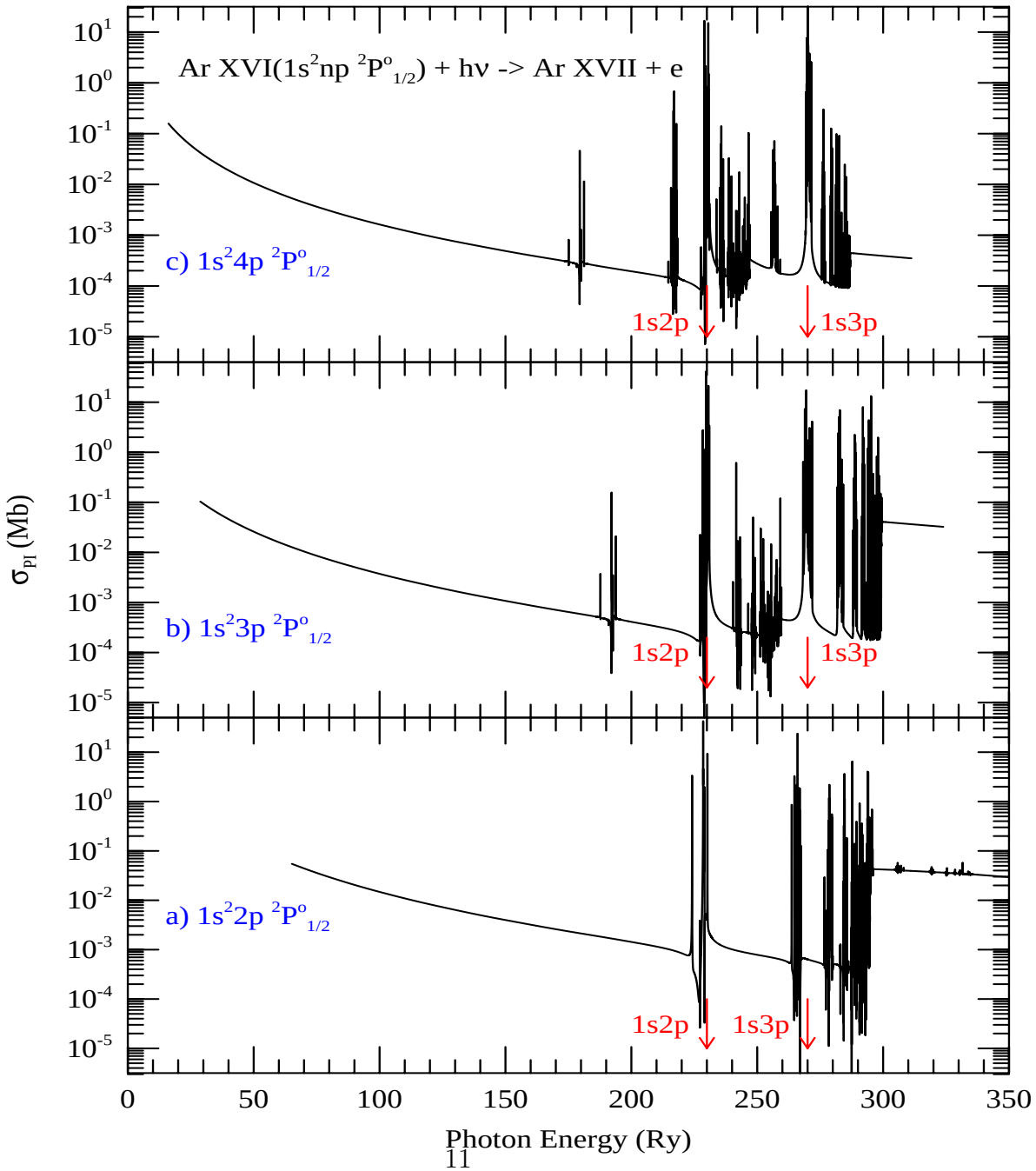

σ_{PI} COMPARISON OF Ar XVII:

- **Total $\sigma_{\rm PI}$ of 1s2s(^{3}S$_1$) state of Ar XVII: a) Under the OP (Fernley et al. 1987), b) Present BPRM**
- **The resonances in b) are due to core excitation in Ar XVII, and the background enhancement is due to 1s-2p excitation of the core. Both effects are missing in the earlier σ_{PI}**

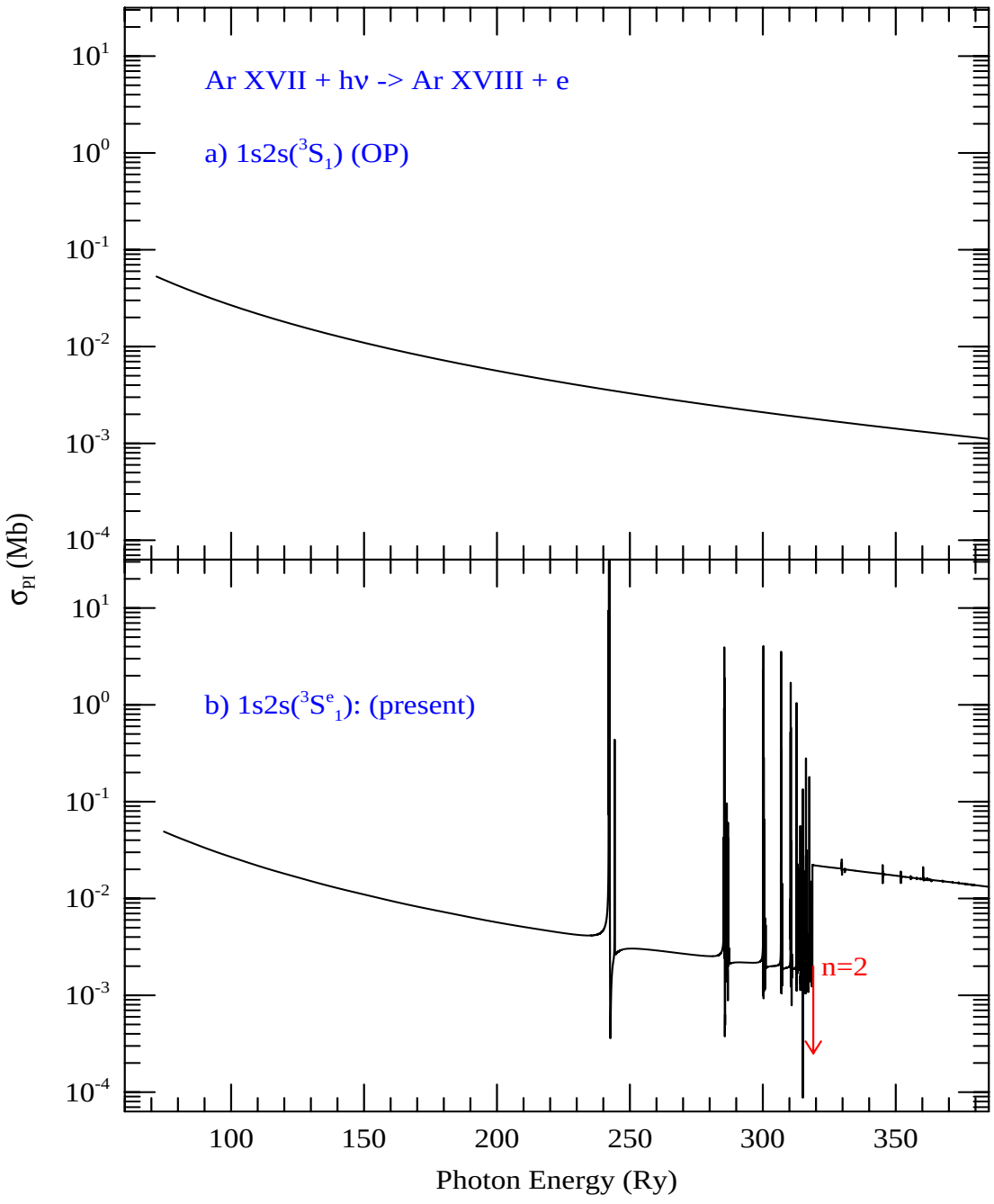

σ_{PI} OF GROUND AND K_α LEVELS OF Ar XVII:

- **a) Total σ_{PI} of gound $1s^2(^1S_0)$ level**
- **b-e) σ_{PI} of four excited (b) $1s2p(^1P_1^o)$-w, (c) $1s2p(^3P_2^o)$-x, (d) $1s2p(^3P_1^o)$-y, (e) $1s2s(^3S_1)$-z levels**
- **The prominent K_α X-ray spectral lines are: (b) resonant w [$1s^2\ (^1S_0) \leftarrow 1s2p(^1P_1^o)$], (c) forbidden x [$1s^2\ (^1S_0) \leftarrow 1s2p(^3P_2^o)$], (d) intercombination y [$1s^2\ (^1S_0) \leftarrow 1s2p(^3P_1^o)$], (e) forbidden z [$1s^2\ (^1S_0) \leftarrow 1s2s(^3S_1)$]; diagnostics for temperature, density, ionization balance, and abundances in plasma sources**
- **Rise in K-shell ionization at n = 2 thresholds is noticed for excited levels, but not for the ground level.**

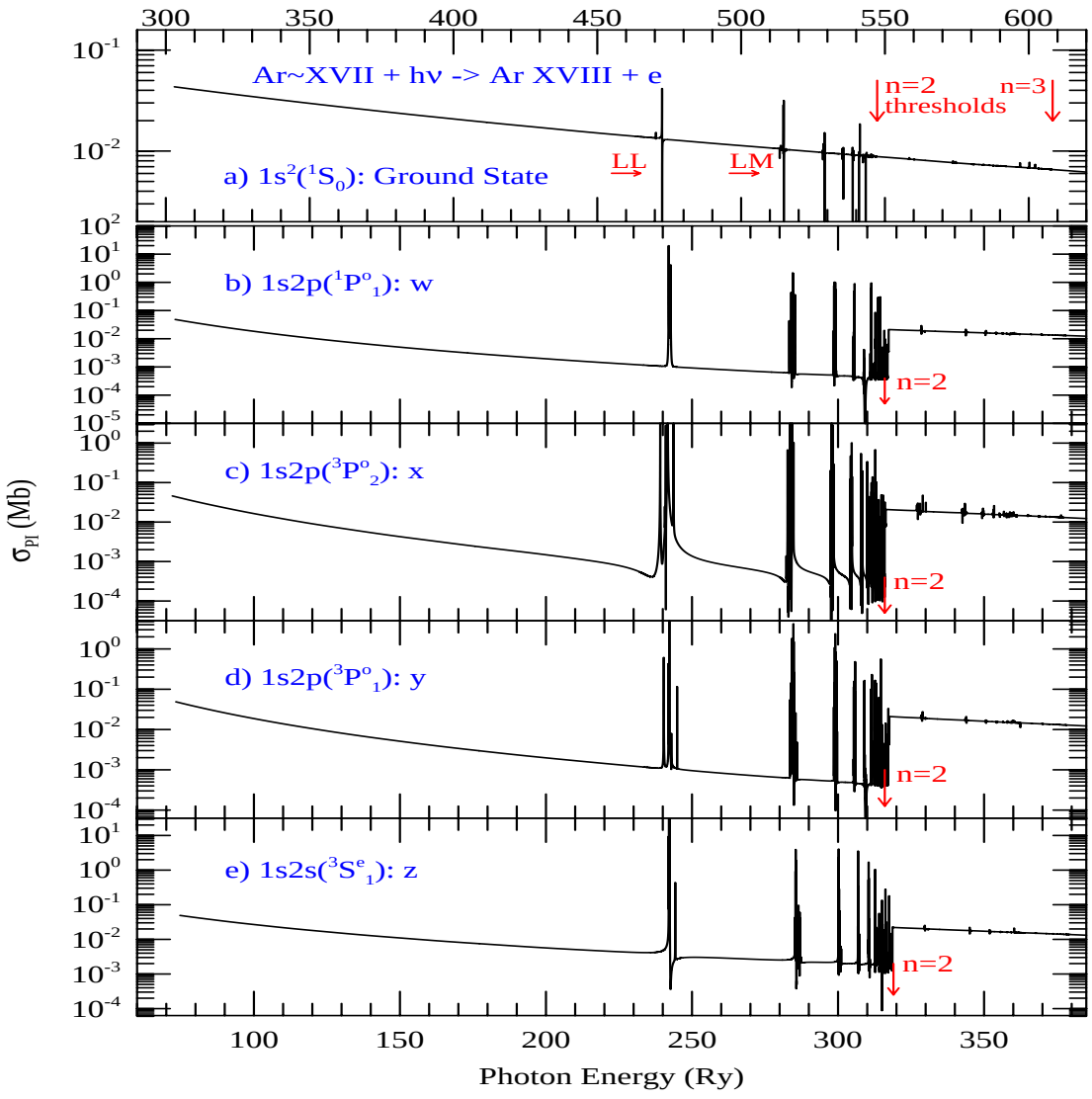

LEVEL-SPECIFIC RRC OF Ar XVII:

- **Unified (e + ion) level-specific recombination rate coefficents (RRC), $\alpha_{\rm RC}(T)$, of the (a) ground and (b-e) four excited levels corresponding to the w, x, y, z diagnostic lines**
- **These are total RRC as both RR and DR are included**
- **While the ground level has smooth $\alpha_{RC}(T)$, most excited levels show a bump due to DR at high T**

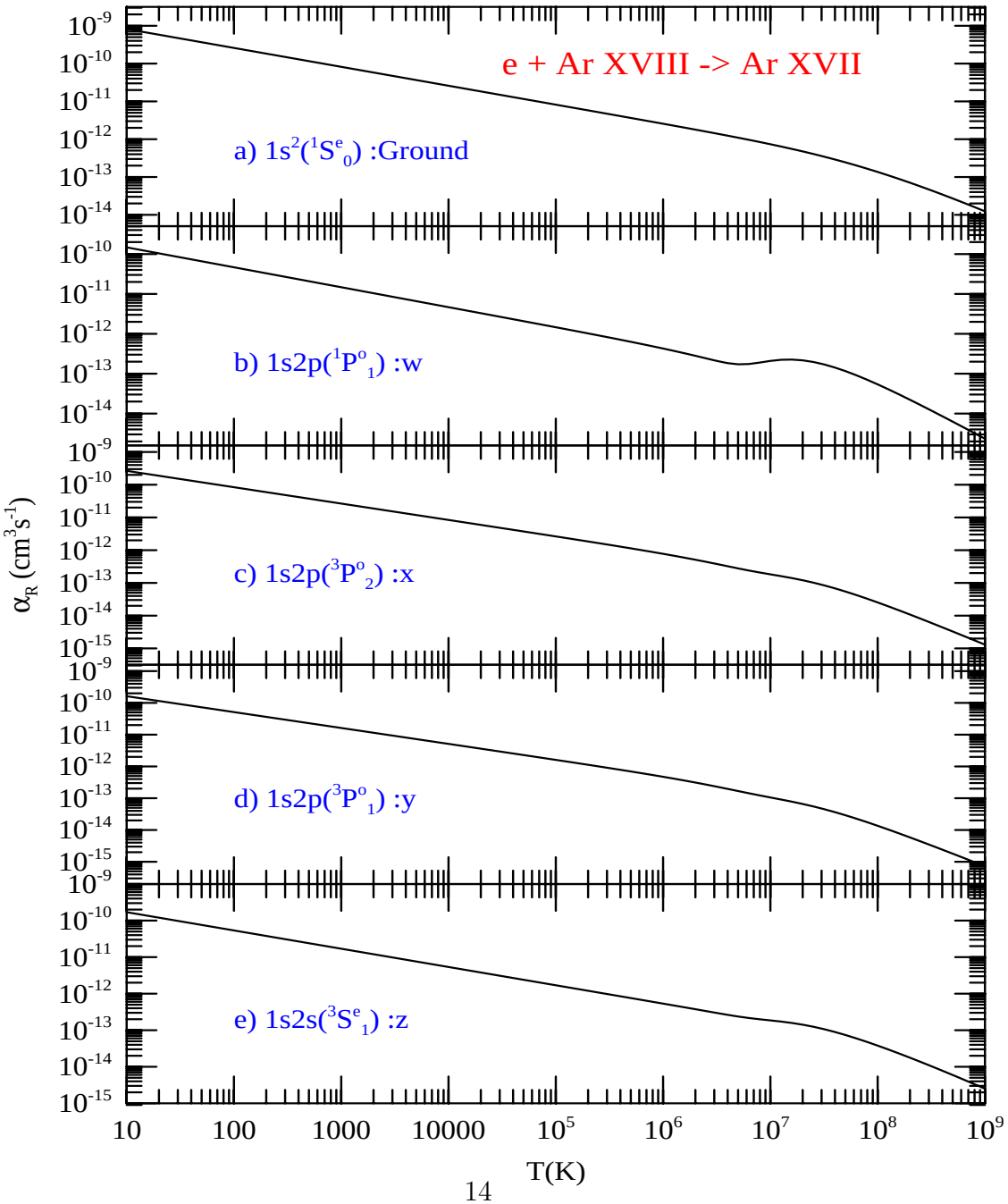

TOTAL $\alpha_R(E)$ OF Ar XVI WITH PHOTO-ELECTRON E:

- **(a) Total unified (e + ion) recombination cross sections, σ_{RC}, and (b) unified recombination rate coefficients, $\alpha_{RC}(E)$, with photoelectron energy - Resonances get weaker with n**
- **Separated resonance complexes, KLL, KLM, etc of n = 2 in $\alpha_{RC}(E)$ (noted in (a)) can be measured experimentally**

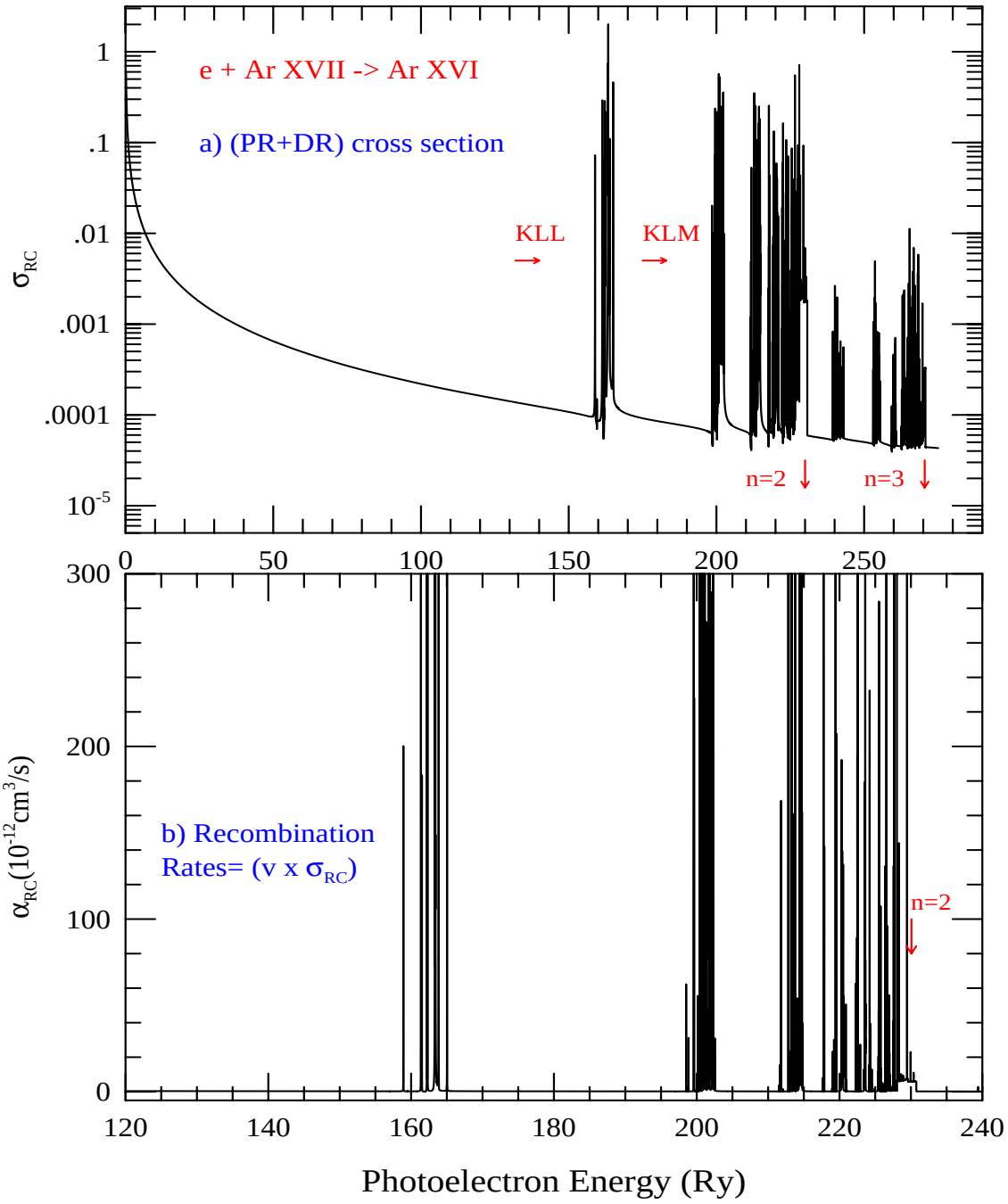

TOTAL RECOMBINATION CROSS SECTION OF Ar XVII:

- **(a) Total unified (e + ion) σ_{RC} and (b) unified recombination rate coefficients, $\alpha_{RC}(E)$ versus photoelectron energy**
- **The resonant complexes, LL, LM, etc of n = 2, MM, MN etc. of n = 3 and those of n = 4 thresholds decrease with n**
- **Resonant complexes, LL, LM, etc of n = 2 thresholds in $\alpha_{RC}(E)$ are measurable**

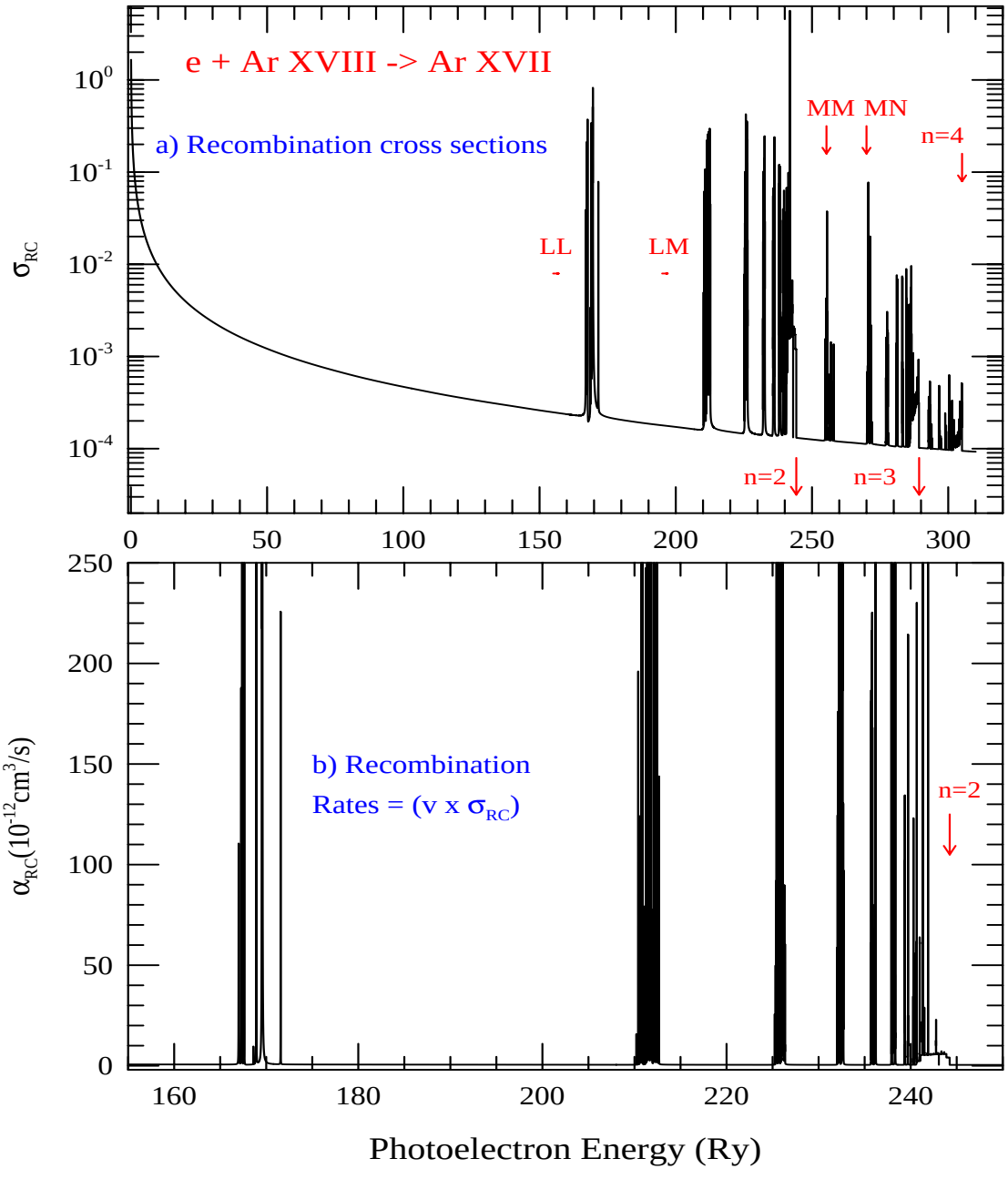

DIELECTRONIC SATELLITE LINES (DES) OF Ar XVI:

- **Dielectronic satellite (DES) lines, in total 22, of in the K_α complex. Top panel: Total spectrum, Bottom panels (3): Resolved and identified lines belonging to final recombined levels - (b) $1s^2 2s(^2S_{1/2})$, (c) $1s^2 2p(^2P^o_{1/2})$, (d) $1s^2 2p(^2P^o_{3/2})$**
- **Because of unified nature of the present method, the shapes and overlapping of the DES lines are produced naturally.**

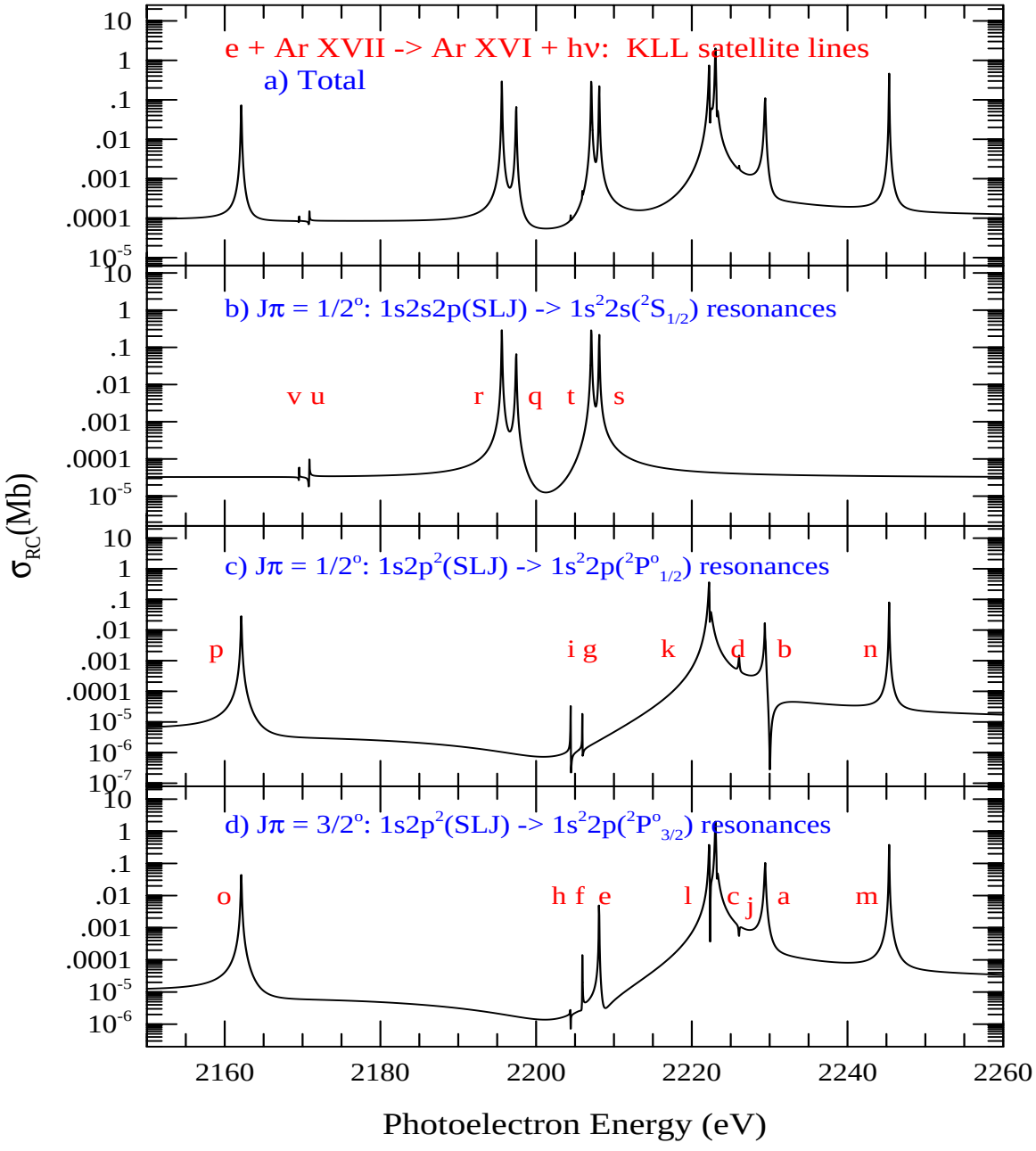

Recombination rate coefficients for dielectronic satellite lines of Ar XVIII forming Ar XVII (notation: x-y $\rightarrow x \times 10^{-y}$).

T(K)	$\alpha_R(cm^3/s)$						
	op	v	u	r	q	ihgft	se
6.1	3.317E-21	6.207E-23	6.170E-23	6.497E-21	2.158E-21	3.934E-23	5.335E-23
6.2	1.415E-19	2.682E-21	2.680E-21	2.953E-19	9.846E-20	1.814E-21	2.472E-21
6.3	2.597E-18	4.976E-20	4.992E-20	5.704E-18	1.907E-18	3.544E-20	4.846E-20
6.4	2.441E-17	4.715E-19	4.746E-19	5.581E-17	1.870E-17	3.500E-19	4.798E-19
6.5	1.348E-16	2.621E-18	2.645E-18	3.182E-16	1.068E-16	2.010E-18	2.762E-18
6.6	4.878E-16	9.534E-18	9.641E-18	1.181E-15	3.971E-16	7.503E-18	1.033E-17
6.7	1.262E-15	2.477E-17	2.509E-17	3.118E-15	1.049E-15	1.990E-17	2.744E-17
6.8	2.502E-15	4.926E-17	4.996E-17	6.280E-15	2.116E-15	4.022E-17	5.552E-17
6.9	4.012E-15	7.920E-17	8.041E-17	1.020E-14	3.439E-15	6.552E-17	9.052E-17
7.0	5.438E-15	1.076E-16	1.093E-16	1.397E-14	4.711E-15	8.992E-17	1.243E-16
7.1	6.450E-15	1.278E-16	1.299E-16	1.670E-14	5.635E-15	1.077E-16	1.490E-16
7.2	6.879E-15	1.365E-16	1.388E-16	1.792E-14	6.051E-15	1.158E-16	1.602E-16
7.3	6.744E-15	1.339E-16	1.363E-16	1.766E-14	5.964E-15	1.142E-16	1.581E-16
7.4	6.184E-15	1.229E-16	1.251E-16	1.626E-14	5.491E-15	1.052E-16	1.457E-16
7.5	5.376E-15	1.069E-16	1.089E-16	1.418E-14	4.790E-15	9.184E-17	1.272E-16
7.6	4.480E-15	8.916E-17	9.081E-17	1.185E-14	4.003E-15	7.678E-17	1.064E-16
7.7	3.611E-15	7.189E-17	7.323E-17	9.567E-15	3.233E-15	6.203E-17	8.595E-17
7.8	2.833E-15	5.643E-17	5.749E-17	7.519E-15	2.541E-15	4.877E-17	6.759E-17
7.9	2.177E-15	4.336E-17	4.418E-17	5.784E-15	1.955E-15	3.753E-17	5.201E-17
8.0	1.644E-15	3.277E-17	3.339E-17	4.374E-15	1.478E-15	2.839E-17	3.934E-17
8.1	1.226E-15	2.443E-17	2.489E-17	3.263E-15	1.103E-15	2.118E-17	2.936E-17
8.2	9.042E-16	1.802E-17	1.836E-17	2.408E-15	8.141E-16	1.563E-17	2.167E-17
8.3	6.613E-16	1.318E-17	1.343E-17	1.762E-15	5.957E-16	1.144E-17	1.586E-17
8.4	4.804E-16	9.577E-18	9.760E-18	1.281E-15	4.330E-16	8.317E-18	1.153E-17
8.5	3.472E-16	6.921E-18	7.054E-18	9.259E-16	3.130E-16	6.012E-18	8.334E-18
8.6	2.498E-16	4.981E-18	5.076E-18	6.664E-16	2.253E-16	4.328E-18	5.999E-18
8.7	1.792E-16	3.572E-18	3.641E-18	4.780E-16	1.616E-16	3.104E-18	4.304E-18
8.8	1.281E-16	2.555E-18	2.604E-18	3.420E-16	1.156E-16	2.221E-18	3.079E-18
8.9	9.147E-17	1.824E-18	1.859E-18	2.441E-16	8.253E-17	1.586E-18	2.198E-18
9.0	6.518E-17	1.300E-18	1.325E-18	1.740E-16	5.881E-17	1.130E-18	1.566E-18

CONCLUSION

1. **Results from ab initio unified method for photoionization and recombination of Ar XVI, Ar XVII, Ar XVIII are presented**
2. **Results includes total and level specific recombination rates and photoionization cross sections of hundreds of bound levels.**
3. **Self-consistent sets of atomic data for photoionization, recombination are obtained and should yield more accurate astrophysical models for diagnostics**
4. **All data will be available on-line at NORAD-Atomic-Data: www.astronomy.ohio-state.edu/nahar∼radiativeatom**